ISSN 1027-4510, Journal of Surface Investigation. X-ray, Synchrotron and Neutron Techniques, 2008, Vol. 2, No. 6, pp. 861–865. © Pleiades Publishing, Ltd., 2008.
Original Russian Text © T.S. Argunova, V.G. Kon, Jung Ho Je, 2008, published in Poverkhnost'. Rentgenovskie, Sinkhrotronnye i Neitronnye Issledovaniya, No. 12, pp. 48–53.

Computer Simulation of Phase-Contrast Images in White Synchrotron Radiation Using Micropipes in Silicon Carbide

T. S. Argunova[a, c], V. G. Kon[b], and Jung Ho Je[c]

[a] *Ioffe Physicotechnical Institute, Russian Academy of Sciences, St. Petersburg, Russia*
[b] *Kurchatov Institute, Russian Research Centre, Moscow, Russia*
[c] *X-ray Image Center, Department of Materials Science and Engineering, Pohang University of Science and Technology, Pohang, Republic of Korea*

Received December 24, 2007

Abstract—A method of computer simulation of phase-contrast images in white synchrotron radiation has been developed to determine the section parameters of micropipes in silicon carbide. The experiments have been carried out using the third-generation synchrotron radiation source the Pohang Light Source (South Korea). The effective spectrum of the synchrotron radiation that forms of an image has been shown to have a relatively sharp maximum at an energy of 16 keV, which makes it possible to conserve coherency within the required limits. A computer program has been developed that automatically determines the diameters of an elliptic section of a micropipe from the condition of coincidence of calculated and experimental profiles. It has been shown that the studied micropipes have a strongly stretched elliptic section that can twist when moving along the pipe axis.

DOI: 10.1134/S1027451008060062

INTRODUCTION

Silicon carbide SiC is a promising semiconductor material for electronic technology. It exceeds silicon in heat conductivity and breakdown voltage and can be used for production of power, high-frequency, and high-temperature devices with small losses. However, the growth of silicon carbide crystals is accompanied by the formation inside it of micropipes in the form of cylindrical pores with diameters from submicrons to several microns. As a rule, micropipes are screw superdislocations with giant Burgers vectors [1, 2]. The micropipe axes are parallel to dislocation lines and their section radii are related to the dislocation Burgers vector [3]. Micropipes induce electrical breakdown in SiC-based devices. They are called killer defects, and their density is among the main quality indexes of a sample.

The study of a micropipe structure in SiC single crystals by nondestructive methods is an important problem. This is necessary both for specialists in crystal growth and for device manufacturers. Micropipes are investigated by different methods including x-ray topography, and optical and scanning electron microscopy [4, 5]. The obtaining of coherent phase-contrast images [6] by synchrotron radiation (SR) is the most direct method for studying the micropipe structure directly inside a sample. Third-generation SR sources have small angular sizes and yield the required space coherence. The SR beam monochromaticity is usually produced by a crystal-monochromator giving a relative width of a spectral line less than 10^{-5} [7, 8]. However, to obtain the image of objects with relatively small cross sections, such a large degree of monochromaticity is not necessary. The images can be obtained by a monochromator with a low resolution [9] or even without a monochromator in a white SR beam [5]. The distribution of micropipes in a sample, their orientation and shape, and reaction between them have been investigated by phase contrast in a white SR beam in [5]. However, to obtain quantitative data on the section sizes and shape of the micropipe, it is necessary to carry out parallel computer simulation of images and to fit theoretical and experimental intensity profiles. Recently, we carried out the first investigation of this kind [10].

In this work, new results of investigation of the micropipe structure in SiC by phase-contrast images in a third-generation SR white beam are presented and the section parameters of micropipes are obtained by fitting of theoretical and experimental intensity profiles. The next section describes the details of the experiment. In the third section, theoretical formulas on the basis of which the computer simulation is carried out are presented and the computer program that automatically searches for the required parameters is described. Results are presented in the fourth section.

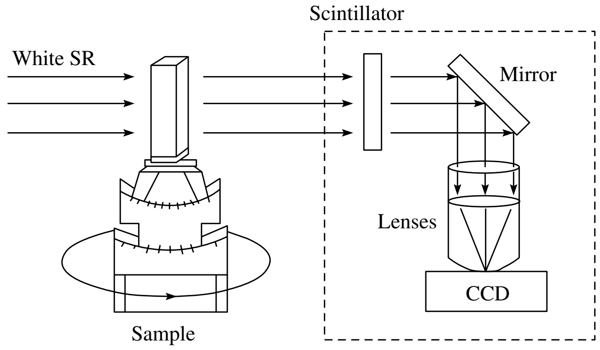

Fig. 1. Experiment circuit.

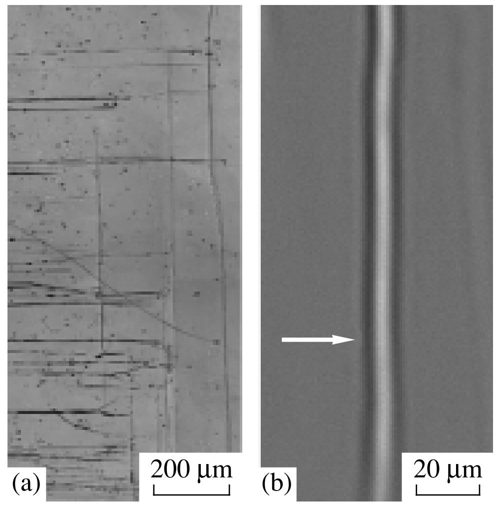

Fig. 2. (a) Optical microphotograph of the sample with micropipes; (b) phase-contrast image of the micropipe turned by 90°.

EXPERIMENTAL

The experiment was carried out at the 7B2 X-Ray Microscopy Station using the third-generation SR source Pohang Light Source (South Korea). The experiment circuit is relatively simple. An SR source is placed far from a sample (34 m). There is nothing between the source and sample except for beryllium windows and a polymer film that hardly affects the SR properties. The source has an effective size of 160 μm in the horizontal direction and 60 μm in the vertical. The experiment circuit is shown in Fig. 1. The sample was installed on a goniometer allowing both rotations about three axes and translations normally to a beam and along it. A $CdWO_4$ crystal scintillator 150 μm thick placed beyond a sample converts radiation into visible light. The image in visible light passes through a lens system, is enlarged, and is recorded by a camera based on charge-coupled devices (CCDs). A camera records the intensity using 14-bit numbers in the form of a matrix consisting of 1600×1200 points (pixels). Image magnification can be controlled in the range from ×1 to ×50 times. In this work, the pixel size was 0.194 μm in terms of an x-ray image.

The recorded micropipe images are very various and depend on many conditions such as the parameters of the SR beam and its spectrum, the section size and shape of a micropipe, the distance from sample to detector, and the micropipe axis orientation relative to a SR beam. The images can have white middle and black edges, black middle and light edges, and can include all intermediate variants. The same pipe changes the contrast when the sample rotates, which indicates a strong angle dependence between a pipe axis and beam. The computer simulation solves the inverse problem, namely the determination of section parameters of a micropipe by fitting of calculated and experimental intensity profiles.

The special sample was prepared for the experiment; it was cut in the form of plate from a 4H-SiC ingot grown by sublimation [11] in an Ar atmosphere at a temperature of 2100°C at a growth rate of 0.5 mm h^{-1}. The plate surface was parallel to the [0001] crystal growth axis and had a thickness of 490 μm. The plate was installed normally to the beam in such a way that the micropipe axis was horizontal. Correspondingly, the intensity profile was recorded in the vertical direction, for which a source had a minimum size. The plate surfaces were polished to remove spurious contrast from a rough surface. To obtain the maximum data set, the images were measured at 11 distances from 5 to 55 cm with a step of 5 cm.

Optical photomicrography of the sample fragment with micropipes is shown in Fig. 2. Dark contrast horizontal lines denote micropipes and more light vertical ones denote inclusions of other polytypes on which micropipes nucleate. The image of the isolated micropipe is shown in the same figure on the right, and the figure is turned by 90° (the pipe axis is horizontal in reality). The arrow shows the place where the intensity profile was recorded. To remove excess details, two patterns were recorded for the sample with micropipes and without them. In the latter case, the sample was replaced by a perfect silicon plate with the same absorption. Then the intensity at each point of the first pattern was divided by that of the second, which is equivalent to contrast subtraction at small contrast regardless of the mean intensity level. However, the intensity profile for the computer simulation was recorded from a small area of the total pattern and the result hardly depended at all on the procedure for removing excess details.

THEORY AND COMPUTER SIMULATION

To calculate phase-contrast images in an SR white beam, it is necessary to know the SR real spectrum in explicit form, which is effectively recorded by a detector. As is known, the initial SR spectrum is wide. Each photon is excited almost instantly and is a coherent superposition of energy harmonics of an optical range up to several hundred keV. Since different photons have random phases and the image is summed over a great number of photons, the real picture can be calculated based on the assumption that different harmonics are noncoherent. In addition, different harmonics have different intensities, which decrease exponentially in an energy range greater than 5 keV. On the other hand, the low energy range is heavily absorbed in all objects placed in the path of the beam including the sample.

As a result, a SR image is effectively formed even in a white beam in a limited energy range which should be calculated taking into account the entire the experiment circuit including the sample. In this sense an image in a white beam is a sum of many pictures obtained for each monochromatic harmonic taking into account the real source size where the picture for individual harmonics is taken with a different specific weight. The SR spectrum used in calculations is shown in Fig. 3. It is seen that the initial spectrum decreases monotonically in the range from 5 to 40 keV, losing almost three orders of magnitude in intensity. Taking into account beryllium windows 2 mm in overall thickness does not strongly change the curve. However, taking into account the absorption in a sample results in a cardinal change. Now the intensity has a maximum at 16 keV and sharply decreases with a decrease in energy. Thus, in spite of the absence of a monochromator, the real spectrum forming an image is localized near 16 keV. It is interesting that the image calculated for 16 keV monochromatic radiation remains, on the whole, the image structure in a white beam. However, note that there is no possibility of changing and, especially, of varying the energy in experiments with an SR white beam.

In the general case, to calculate a monochromatic image, a micropipe can be represented as a quasilinear object in which the electron density changes quickly across the axis and slowly along it. Separating the profile of relative intensity $I(x)$ in some section across the axis, the dependence along the axis can be neglected. In this approximation, the intensity is described in the following way:

$$I(x) = |a(x_0)|^2,$$
$$a(x_0) = \int dx_1 P_K(x_0 - x_1, Z)T(x_1), \quad x_0 = x\frac{z_0}{z_t}, \tag{1}$$

where z_0 is the distance between a source and an object, and z_1 is the distance from an object to a detector, $z_t = z_0 + z_1$, $Z = z_0 z_1 / z_t$. Thus, the task is reduced to calculating the convolution of two functions.

The first of these is the Kirchhoff propagator,

$$P_K(x, z) = \frac{1}{(i\lambda z)^{1/2}}\exp\left(i\pi\frac{x^2}{\lambda z}\right), \tag{2}$$

which corresponds to a reduced distance Z. Here λ is the monochromatic radiation wavelength. The propagator describes coherent wave transport through the vacuum. The second function $T(x)$ describes the effect of an object on a coherent wave. Since an object has a small longitudinal size, it is quite sufficient to take into account the change in the wave phase and amplitude within the geometrical optics without taking into account the change in beam trajectory, assuming that all beams are parallel to the z axis. In this approximation, we can exclude, for simplicity, the uniform part of a sample in a material with an elliptic section and take into account only wave distortion caused by nonuniformity. Then $T(x) = 1$ at $|x| > R$ and

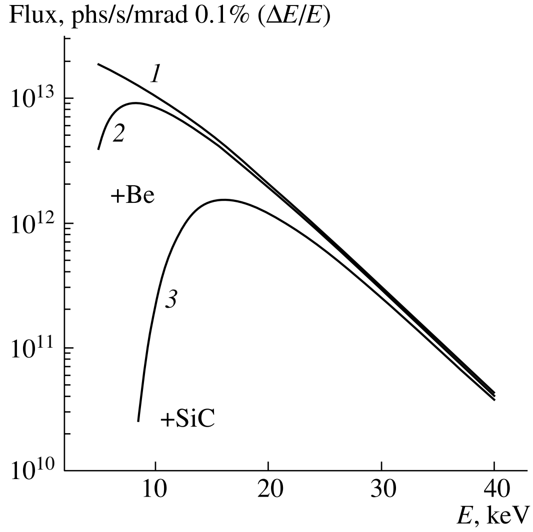

Fig. 3. Effective synchrotron radiation spectrum recorded by a detector: (*1*) initial spectrum; (*2*) after absorption in beryllium windows; (*3*) after additional absorption in the sample.

$$T(x) = \exp\left[(iP + M)\left(1 - \frac{x_2}{R^2}\right)^{1/2}\right],$$
$$P = \frac{2\pi}{\lambda}\delta R_0, \quad M = P\frac{\beta}{\delta}. \tag{3}$$

at $|x| < R$. Here R and R_0 are the radii of an elliptic section of a micropipe across a beam (along the x axis) and along a beam (along the z axis). Their double values, i.e., the diameters of the elliptic section, are a priori unknown and are the quantities sought.

Since the integrand in (1) does not decrease at infinity, subject to the propagator property, the integral was reduced for numerical calculations to the following form:

$$a(x_0) = 1 + \int dx_1 P_K(x_0 - x_1, Z)[T(x_1) - 1]. \tag{4}$$

The intensity profiles were calculated for 71 harmonics in the energy range from 5 to 40 keV with a constant step of 0.5 keV and then summed with allowance for the spectrum shown in Fig. 3. The computer simulation was carried out using the FIMTIM program written in the ACL language [12] and operating under the control

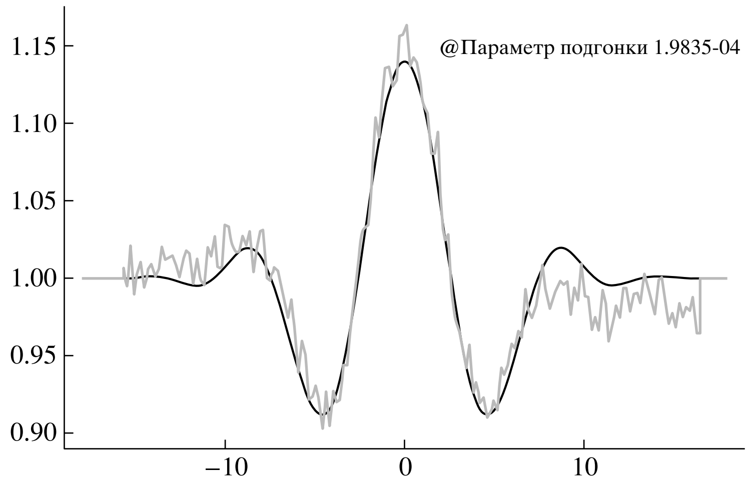

Fig. 4. Typical graph recorded by the FIMTIM program during fitting of the section parameters of the micropipe. The distance between the detector and sample is 45 cm. The smooth curve is the theoretical calculation; the broken line is the experiment taking into account unavoidable noise.

of an interpreter written in the Java language. Convolution (4) was calculated by double Fourier transform using the fast Fourier transform algorithm [13]. The calculation was carried out using a net consisting of 4096 points (2048 points were used in the automatic fit mode) and the area was the input parameter (usually 34 μm). The program read the normalized experimental intensity profile, calculated the profile by Eqs. (1) and (4) for the specified values of R and R_0, interpolated the experimental profile to the points of the calculated net, and calculated the sum of squared deviations. A graph of experimental and calculated profiles was filed at each step. A typical example of a graph is shown in Fig. 4. The task was to obtain the best coincidence of curves by varying the values of parameters R and R_0. Note that this was often obtained with a good accuracy. The parameters can be varied both manually and automatically. The former calculated all points in the square net. The latter carried out a search calculating the points nearest to the required one at each step and shifting to the point with the best coincidence. In this case previously calculated points were not recalculated.

DISCUSSION AND CONCLUSIONS

As is known, the coherent phase-contrast image of a transparent object does not describe an object directly and is in fact a special type of hologram. In this case, the image of the same object at different distances, firstly, increases and, secondly, changes its structure. For this reason, it has been proposed in [10] to compare the total image set of the same micropipe at different distances. In this case, it has been assumed that the micropipe itself has a cylindrical section and the average radius of this section was virtually determined.

However, the subsequent, more subtle analysis by the FIMTIM program has shown that the assumption of a cylindrical section is not always true. The studied micropipe can have a strongly stretched elliptic section, and, moreover, this section can turn in certain places when moving along the pipe axis. On the other hand, the experimental recording of the same section at different distances under these conditions requires the very fine adjustment of the experiment scheme. Otherwise the shifts of an image along the axis are inevitable with changing distance. For this reason it is necessary to fit the section parameters individually for each distance. If the parameters are correctly determined, they should not depend on distance. In this approach, the independence of the parameters from distance is a criterion both of the correctness of the statement of experiment and of the fitting procedure.

Figure 5 shows the section diameters of a micropipe determined by fitting from the data obtained at different distances for three close sections in the area of the image denoted by the arrow in Fig. 2. It is seen that the obtained parameters change weakly both as a function of distance and with a small shift of the section along the axis. However, the longitudinal diameter of a micropipe is only 1 μm, whereas the transverse diameter is 5 μm. This result is rather unexpected and has been obtained for the first time. Moreover, examining the other image area, we found an interesting effect in which a micropipe is twisted, whereby its section changes the parameters as it moves along the pipe axis. Figure 6 shows the section diameters as a function of position of sections along the pipe axis obtained for distances of 45 and 55 cm. Though the accuracy in determining the parameters is low, it has been reliably observed that the pipe in some areas has an elliptic section that has been strongly stretched along the beam with a transverse diameter of 0.5 μm and a longitudinal

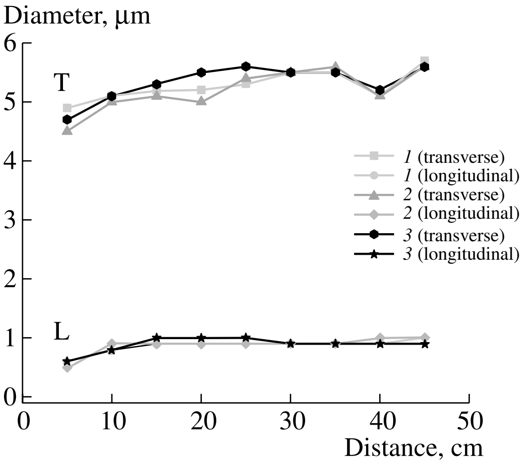

Fig. 5. Section parameters of the micropipe determined from the images at different distances from the sample and for three close sections along the pipe axis with numbers 1–3. *T* denotes transverse diameters and *L* denotes longitudinal diameters.

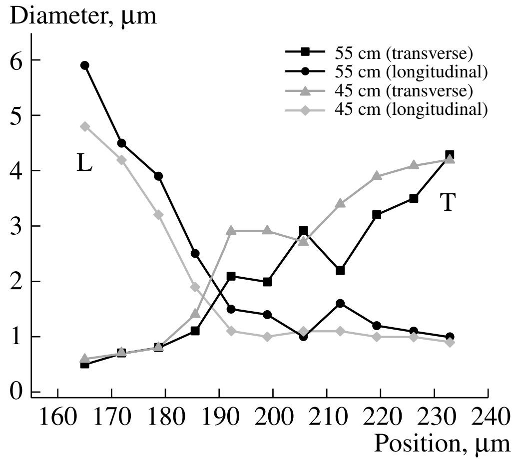

Fig. 6. Section parameters of the micropipe for different points along the pipe axis determined from the images at the distance from the sample of 55 and 45 cm. *T* denotes transverse diameters and *L* denotes longitudinal diameters.

diameter of 5.5 μm, which turns rather quickly (on an area of 80 μm in length) across the beam.

The results allow us to conclude that the computer simulation method is effective when the sectional structure of micropipes in silicon carbide is determined by phase-contrast images in an SR white beam. In this case, it is possible not only to obtain the real parameters but to also fix their dynamics when moving along the micropipe axis. We believe that further development of this method make it possible to improve the reliability and validity of results.

ACKNOWLEDGMENTS

V.G.K. acknowledges the support of the Russian Foundation for Basic Research (projects nos. 05-02-16702, 07-02-00067) and the RF Presidential Program in Support of Leading Scientific Schools (NSh 6869–2006–2). The experimental part of the work was supported by the project Creative Research Initiatives (Functional X-ray Imaging) of MOST/KOSEF and by the Russian Foundation for Basic Research, project no. 06–02–16244.

SPELL OK

REFERENCES

1. P. Krishna, S.-S. Jiang, and A. R. Lang, J. Cryst. Growth **71**, 41 (1985).
2. X. R. Huang, M. Dudley, W. M. Vetter, et al., Appl. Phys. Lett. **74**, 353 (1999).
3. F. C. Frank, Acta Crystallogr. **4**, 497 (1951).
4. I. Kamata, H. Tsuchida, T. Jikimoto, and K. Izumi, Jpn. J. Appl. Phys. Part 1 **39**, 6496 (2000).
5. M. Yu. Gutkin, A. G. Sheinerman, T. S. Argunova, et al., J. Appl. Phys. **100**, 093518 (2006).
6. A. Snigirev, I. Snigireva, V. Kohn, et al., Rev. Sci. Instrum. **66**, 5486 (1999).
7. P. Cloetens, R. Barrett, J. Baruchel, et al., J. Phys. D: Appl. Phys **29**, 133 (1996).
8. S. Milita, R. Madar, J. Baruchel, et al., Mater. Sci. Eng. **61–62**, 63 (1999).
9. Y. Hwu, H. H. Hsieh, M. J. Lu, et al., J. Appl. Phys. **86**, 4613 (1999).
10. V. G. Kohn, T. C. Argunova, and Ho Je Jung, Appl. Phys. Lett. **91**, 171901 (2007).
11. Yu. A. Vodakov, A. D. Roenkov, M. G. Ramm, et al., Phys. Stat. Solidi B **202**, 177 (1997).
12. http://vkacl.narod.ru.
13. N. S. Bakhvalov, *Numerical Methods* (Nauka, Moscow, 1973) [in Russian].